Seismic isolation of buildings by using metamaterials

Stefania Fiore[a,f] , Vincenzo Carbone[b], Antonio Madeo[a], Francesca Garescì[c], Massimo Chiappini[d,f], Giovanni Finocchio[e,f]
[a] *Dipartimento di Ingegneria Informatica, Modellistica, Elettronica e Sistemistica, University of Calabria, Italy*
[b]*Dipartimento di Fisica, University of Calabria, Italy*
[c]*Dipartimento di Ingegneria , University of Messina, Italy*
[d] *Istituto Nazionale di Geofisica e Vulcanologia (INGV), Roma, Italy*
[e] *Department of Mathematical and Computer Sciences, Physical Sciences and Earth Sciences, University of Messina, Italy*
[f] *Monitoraggio Ambientale e Ricerca Innovativa Strategica Scarl, Roma, Italy*

Keywords: metamaterial; isolation; reduction of spectral acceleration; seismic response.

ABSTRACT
The idea of metamaterials, developed in electromagnetic theory, has been extended to earthquake engineering with the concept of seismic metamaterial (Finocchio et al., 2014). Among the possible strategies, recently it has been shown that composite foundations (CFs), integrating the physics of seismic metamaterials into a foundation of a building, are promising for the seismic isolation of new buildings (Casablanca et al., 2018). The macroscopic dynamical behavior of the CF, which can be modeled as a periodic chain of mass-in-mass systems, depends on its intrinsic properties, such as the internal resonance frequency.
Here, we have studied seismic local response analyses of layered soil described by Kelvin-Voigt model, both in time and frequency domain, where the CF is integrated within the soil. The real accelerograms, spectrum-compatible, are used as inputs for the analyses. The resulting dynamics are described by lumped parameters and the stationary elastic solution is evaluated numerically. In the end, acceleration response spectra are calculated. These response spectra are key tools to design civil structures and used as the main design instruments in the current technician rules.
Results of calculations show that the presence of metamaterials within the soil significantly reduces the amplification function of the system. At the same time, the response spectrum shows attenuation in the spectral quantities.

1 COMPOSITE FOUNDATION

The concept of 'composite foundation' (CF) has been introduced by (Casablanca et al., 2018) as a new generation of seismic isolation devices combining together the physics of seismic metamaterials and the structural function of the foundation of the building. The CF has the property to preserve large stiffness for normal actions (compression) and low stiffness for shear actions. It has been demonstrated that the CF can be modelled properly as a periodic chain of mass-in-mass unit cells and, using Bloch's theorem, the dispersion relationship can be computed so that the band-gap should be estimated between (it is between 5 Hz and 14 Hz with the parameters used by (Casablanca et al., 2018). An experimental proof of the working principle of the CF has been already published (Casablanca et al., 2018), where the CF is composed by four concrete plates with internal resonators. The experimental data have shown a considerable attenuation within the band-gap opening a direction for a potential application in the realization of new buildings. Here we extend the previous work by considering a study involving soil, metamaterials and a building altogether. .

2 MECHANICAL MODEL

One-dimensional mechanical model is used to estimate the horizontal accelerations of the soil. They are defined within the following hypotheses: (i) soil rest on bedrock, (ii) horizontal stratification, (iii) lateral confinement soil is

neglected, (iv) vertical propagation direction of shear waves (Snell's low) (Kramer, 1996).

2.1 Discrete model for the soil

The Voigt's model is used to describe the viscous-elastic response of the soil. If the external force *F* is applied, the equilibrium condition is expressed in equation :

$$F = k\sigma + c\frac{\partial \sigma}{\partial t}$$

where σ is the stress component, *k* and *c* are the stiffness and damping coefficients as illustrated in Figure 1.

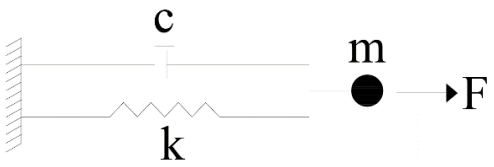

Figure 1. Mechanical viscous-elastic Voigt's model.

Layers of soil are modelled as lumped masses connected each other with springs (elements with elastic stiffness) and damper (elements with viscous damping) as illustrated in Figure 2. The lumped parameters *m*, *c* and *k* are calculated from geotechnical correlations (Lanzo, 1999). For the j^{th} layer the parameters are shown in equation , where γ is the specific weight, *h* the layer's height, *G* the stiffness shear modulus and *η* the viscous coefficient.

$$m_j = \frac{\gamma_{j-1}h_{j-1} + \gamma_j h_j}{2}, \quad k_j = \frac{G_j}{h_j}, \quad c_j = \frac{\eta_j}{h_j}$$

The stiffness shear modulus variation with depth is evaluated with the equation , where v_0 is the wave velocity at the top, α the heterogeneity coefficient and *H* the total height of considered soil. Viscosity factor expressed in equation depends on the forcing pulsation.

$$G_j = \gamma_j \left[v_0 \left(1 + \alpha \frac{z_j}{H} \right) \right]^2$$

$$\eta_j = \frac{2G_j D_j}{\omega}$$

Similar approaches are already used in commercial software for local seismic response analyses (Lanzo, Pagliaroli, & D'Elia, 2003), (Lo Presti, Lai, & Puci, 2006). If the external excitement is a seismic horizontal acceleration, applied as an accelerogram $a_g(t)$, the equilibrium condition for the j^{th} layer is given by equation .

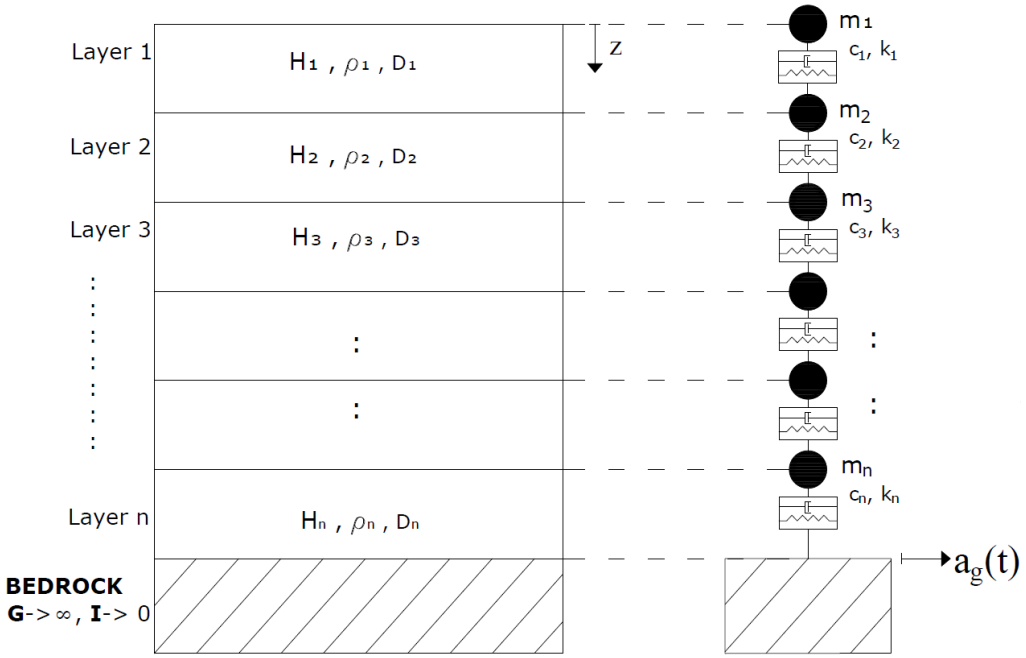

Figure 2. Soil model with lumped parameters in comparison with the continuum model of layered soil.

$$m_j\left(\ddot{u}_j+\iota_j a_g\right)+c_j\left(\dot{u}_j-\dot{u}_{j+1}\right)+c_{j-1}\left(\dot{u}_j-\dot{u}_{j-1}\right)+k_j\left(u_j-u_{j+1}\right)+k_{j-1}\left(u_j-u_{j-1}\right)=0$$

$$p_{eff,j}=-m_j\iota_j a_g$$

$$m_j\ddot{u}_j+c_j\left(\dot{u}_j-\dot{u}_{j+1}\right)+c_{j-1}\left(\dot{u}_j-\dot{u}_{j-1}\right)+k_j\left(u_j-u_{j+1}\right)+k_{j-1}\left(u_j-u_{j-1}\right)=p_{eff,j}$$

where ι_j is the j[th] component of drag vector (**I**) that allows to apply seismic acceleration on each degree of freedom of the system. Using the quantity in equation , i.e. seismic effective force (Anil K. Chopra, 2013), the equilibrium equation can be rewritten as .

2.2 Discrete model for metamaterial

Mass-in-mass unit cell represents a mechanical model to describe a structure composed by external matrix with inclusions (Chatzi, Dertimanis, Antoniadis, & Wagner, 2016; Huang & Sun, 2009). The mass-in-mass unit cell model is studied extensively, continuum models are presented including the presence of negative effective dynamical mass within the frequencies of the band-gap (Huang & Sun, 2009; Huang, Sun, & Huang, 2009; Tan, Huang, & Sun, 2012; Zhou, Wei, & Tang, 2016).

For each mass-in-mass unit, the cell parameters are m^i, m^e, k^i, k^e, c^i, c^e and the dynamic solution is described with two horizontal displacements (u^i, u^e). The CF is then modelled with a chain of mass-in-mass unit cells connected each other with external springs and damping as illustrated in Figure 3.

For each mass-in-mass unit cell the parameters describe the single plate of metamaterial as shown in Figure 4.

The contains the equilibrium equations for the unit cell j^{th}.

In the present work, layers of metamaterial have been considered as integrated within the soil, while the damping coefficients of the unit cell (c^i, c^e) are evaluated from D^i_j that is the internal damping factor (high damping due to rubber) and D^e_j, the external damping factor (ultra-low damping layer between plates).

$$\begin{cases} m_j^i\ddot{u}_j^i+c_j^i\left(\dot{u}_j^i-\dot{u}_j^e\right)+k_j^i\left(u_j^i-u_j^e\right)=p_{eff,j}^i \\ m_j^e\ddot{u}_j^e+c_j^i\left(\dot{u}_j^e-\dot{u}_j^i\right)+c_{j-1}^e\left(\dot{u}_j^e-\dot{u}_{j-1}^e\right)+c_j^e\left(\dot{u}_j^e-\dot{u}_{j+1}^e\right)+\dots \\ \qquad \dots+k_j^i\left(u_j^e-u_j^i\right)+k_{j-1}^e\left(u_j^e-u_{j-1}^e\right)+k_j^e\left(u_j^e-\dot{u}_{j+1}^e\right)=p_{eff,j}^e \end{cases}$$

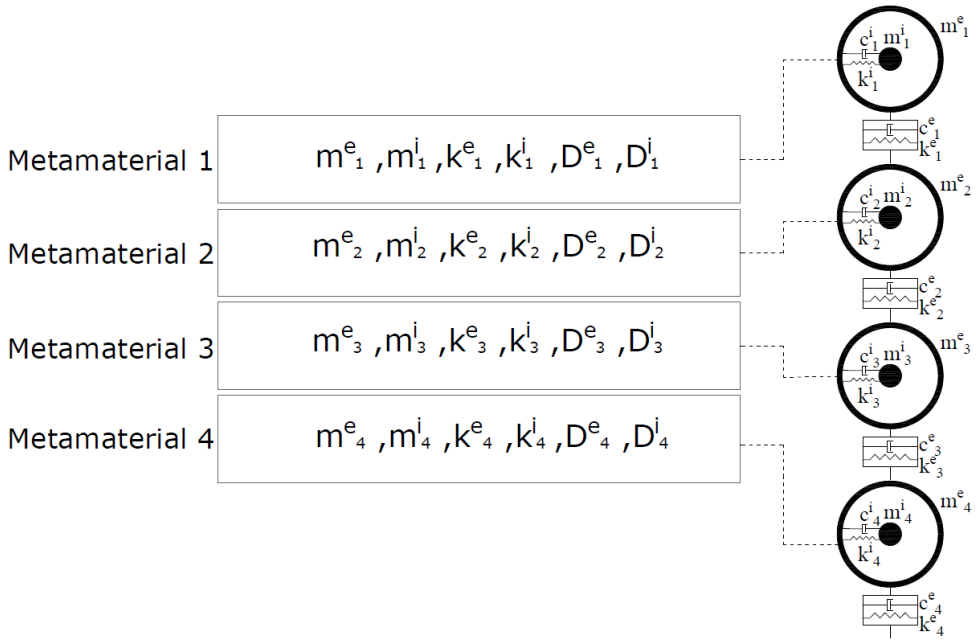

Figure 3. Plates of metamaterial overlapped modelled with a chain of mass-in-mass unit.

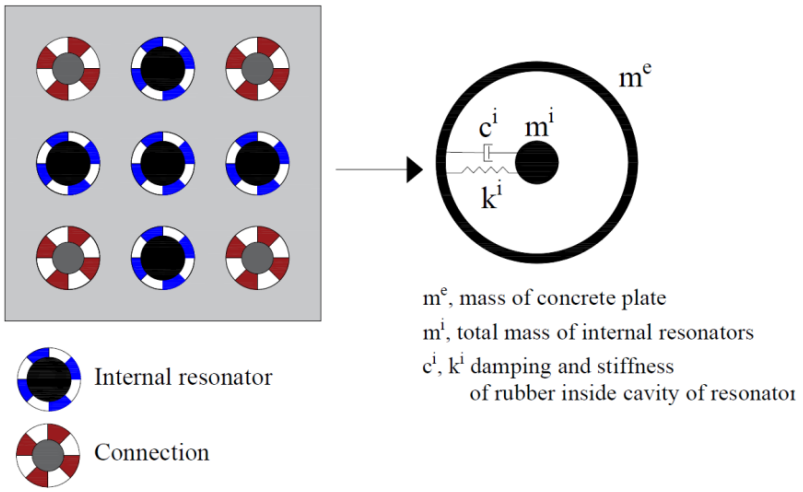

Figure 4. On the left the constructive scheme of the single plate of metamaterial is illustrated, and on the right the scheme of a mass-in-mass unit cell is shown.

2.3 Seismic input: accelerograms

Recorded earthquake signals are usually supplied as acceleration time-history from which it is possible to estimate both duration and peak ground acceleration. Moreover a seismic signal contains a rich spectrum that can be characterized by the main excitation frequencies and their power of the Fourier spectrum of the accelerogram. .

In a linear approximation, some parameters vary with the excitation frequency of the system , therefore an accelerogram requires decomposition in its harmonics. *Fourier Discrete Transform* allows decomposition of signal into several harmonic components (Robert A. Witte, 1993). For a given time signal, which is sampled in N points at a distance t_0, the Fourier Transform (*F*) is given by $A(\omega)$, as indicated in (1.9)(1.10):

$$F(a(t)) = A(\omega)$$

$$A(\omega) = \sum_{n=0}^{N-1} a(nt_0) e^{i\, n\, \omega t_0}$$

2.4 Solution

Using mass-in-mass unit cell for layers of metamaterial (N_{sm}) and mass-spring-damping unit cell for layers of soil (N_g), the dimension of the dynamic system is:

$$DOFs = 2N_{sm} + N_g$$

Variables of the system are:

$$u_1^i, u_1^e, u_2^i, u_2^e, \ldots, u_{N_{sm}}^i, u_{N_{sm}}^e, u_1, u_2, u_3, \ldots u_{Ng}$$

Re-ordered as:

$$u_1, u_2, u_3, \ldots, u_k, \ldots u_N \quad with \quad N = 1 \ldots DOFs$$

The drag vector is:

$$\boldsymbol{I} = [1,1,\ldots,1]^T, \quad \dim(\boldsymbol{I}) = Nx1$$

System of equations can be express in compact notation using matrices and vectors where **M** is the mass matrix, $\boldsymbol{C}$ is damping matrix, **K** is the stiffness matrix and $\boldsymbol{P_{eff}}$(t) is an effective seismic force vector. Indicating with h=2N_{sm} and N= DOFs, matrices and vectors quantities are shown as follows.

$$\boldsymbol{M}\ddot{\boldsymbol{u}}(t) + \boldsymbol{C}\dot{\boldsymbol{u}}(t) + \mathbf{K}\,\mathbf{u}(t) = \boldsymbol{P_{eff}}(t)$$

$$\boldsymbol{M} = \begin{bmatrix} m_1 & & & & \\ & m_2 & & & \\ & & \ddots & & \\ & & & \ddots & \\ & & & & m_N \end{bmatrix}, \quad \boldsymbol{P_{eff}}(t) = -\boldsymbol{M}\,\boldsymbol{I}\,a_g(t) = -\begin{Bmatrix} m_1 \\ m_2 \\ \vdots \\ m_k \\ \vdots \\ m_N \end{Bmatrix} a_g(t)$$

$$\boldsymbol{K} = \begin{bmatrix}
k_1 & -k_1 & 0 & \cdots & \cdots & & & & & & 0 \\
-k_1 & k_1+k_2 & 0 & -k_2 & 0 & \cdots & & & & & 0 \\
0 & 0 & k_3 & -k_3 & 0 & \cdots & & & & & 0 \\
\vdots & -k_2 & -k_3 & k_2+k_3+k_4 & 0 & -k_4 & 0 & \cdots & & & 0 \\
\vdots & \ddots & \ddots & \ddots & \ddots & \ddots & \ddots & & & & \vdots \\
\vdots & & & 0 & 0 & k_{h-1} & -k_{h-1} & 0 & \cdots & & 0 \\
\vdots & & & & -k_{h-2} & -k_{h-1} & k_{h-1}+k_h+k_{h+1} & -k_{h-2} & 0 & \cdots & 0 \\
\vdots & & & & & 0 & -k_{h+1} & k_{h+1}+k_{h+2} & -k_{h+2} & 0 & \cdots & 0 \\
\vdots & & & & & & 0 & -k_{h+2} & k_{h+2}+k_{h+3} & -k_{h+3} & 0 & \cdots 0 \\
\vdots & & & & & & \ddots & \ddots & \ddots & \ddots & & \vdots \\
\vdots & & & & & & & 0 & -k_{N-2} & k_{N-2}+k_{N-1} & -k_{N-1} & \\
0 & 0 & 0 & 0 & 0 & 0 & 0 & 0 & 0 & -k_{N-1} & k_N &
\end{bmatrix}$$

$$\boldsymbol{C}=\begin{bmatrix}
c_1 & -c_1 & 0 & \cdots & \cdots & & & & & & 0\\
-c_1 & c_1+c_2 & 0 & -c_2 & 0 & \cdots & & & & & 0\\
0 & 0 & c_3 & -c_3 & 0 & \cdots & & & & & 0\\
\vdots & -c_2 & -c_3 & c_2+c_3+c_4 & 0 & -c_4 & 0 & \cdots & & & 0\\
\vdots & \ddots & \ddots & \ddots & \ddots & \ddots & \ddots & & & & \vdots\\
\vdots & & & 0 & 0 & c_{h-1} & -c_{h-1} & 0 & \cdots & & 0\\
\vdots & & & & -c_{h-2} & -c_{h-1} & c_{h-1}+c_h+c_{h+1} & -c_{h-2} & 0 & \cdots & 0\\
\vdots & & & & & 0 & -c_{h+1} & c_{h+1}+c_{h+2} & -c_{h+2} & 0 & \cdots & 0\\
\vdots & & & & & & 0 & -c_{h+2} & c_{h+2}+c_{h+3} & -c_{h+3} & 0 & \cdots & 0\\
\vdots & & & & & & & \ddots & \ddots & \ddots & \ddots & & \vdots\\
\vdots & & & & & & & & 0 & -c_{N-2} & c_{N-2}+c_{N-1} & -c_{N-1} & \\
0 & 0 & 0 & 0 & 0 & 0 & 0 & 0 & 0 & -c_{N-1} & c_N &
\end{bmatrix}$$

$$\ddot{\boldsymbol{u}}(t)=\begin{Bmatrix}\ddot{u}_1\\ \ddot{u}_2\\ \vdots\\ \ddot{u}_k\\ \vdots\\ \ddot{u}_N\end{Bmatrix},\qquad \dot{\boldsymbol{u}}(t)=\begin{Bmatrix}\dot{u}_1\\ \dot{u}_2\\ \vdots\\ \dot{u}_k\\ \vdots\\ \dot{u}_N\end{Bmatrix},\qquad \boldsymbol{u}(t)=\begin{Bmatrix}u_1\\ u_2\\ \vdots\\ u_k\\ \vdots\\ u_N\end{Bmatrix}$$

System of equations is stationary and linear.

3 NUMERICAL INVESTIGATION

In this work, a numerical study has been performed to validate the one-dimensional model with lumped parameters. This model is used to investigate the behaviour of the CF in a real application and to calculate some engineering quantities explaining characterizing the effective attenuation of seismic effects.

3.1 Input for seismic dynamic analysis

A set of seven real acceleration time-history, scaled at peak ground acceleration, as indicated by standards (EC8-1), has been used for the dynamical analyses. In particular, we have considered real accelerograms recorded on outcropping bedrock, spectrum-compatible, on average, with code spectra (in Italy NTC08), obtained by software SEISM-HOME based on ASCONA method for selection of compatible natural accelerograms(Corigliano, Lai, Rota, & Strobbia, 2012). Data are collected in Table 1 and 2.

Table 1. Study site and return period (RP) of design earthquake.

Site	Lat	Long	RP
Messina	38.2660	15.5240	475

In Table 2, the parameters of the earthquakes are the moment magnitude, which is the energy content of the event, and the epicentral distance between the wave sources and the measuring station. Scaling factor makes spectrum-compatible the real record, according to the design return period.

Table 2. Earthquake related quantities for each accelerogram of the study set. Abbreviations indicate: Moment

magnitude(Mw), epicentral distance(E-Dist) and scaling factor(SF).

	Mw	E-Dist (Km)	SF
Nr 1	6.87	11.00	0.64
Nr 2	6.20	32.00	2.78
Nr 3	6.93	94.31	2.34
Nr 4	6.69	61.79	2.18
Nr 5	6.60	36.18	1.70
Nr 6	6.00	33.00	1.45
Nr 7	6.30	101.74	0.67

Figure 5 shows each accelerogram, in time domain $a(t)$ and in frequency domain $A(\omega)$. The first representation allows to estimate significant duration and the peak acceleration of each event whereas the second points out the main excitement frequency and how wide the frequency band is.

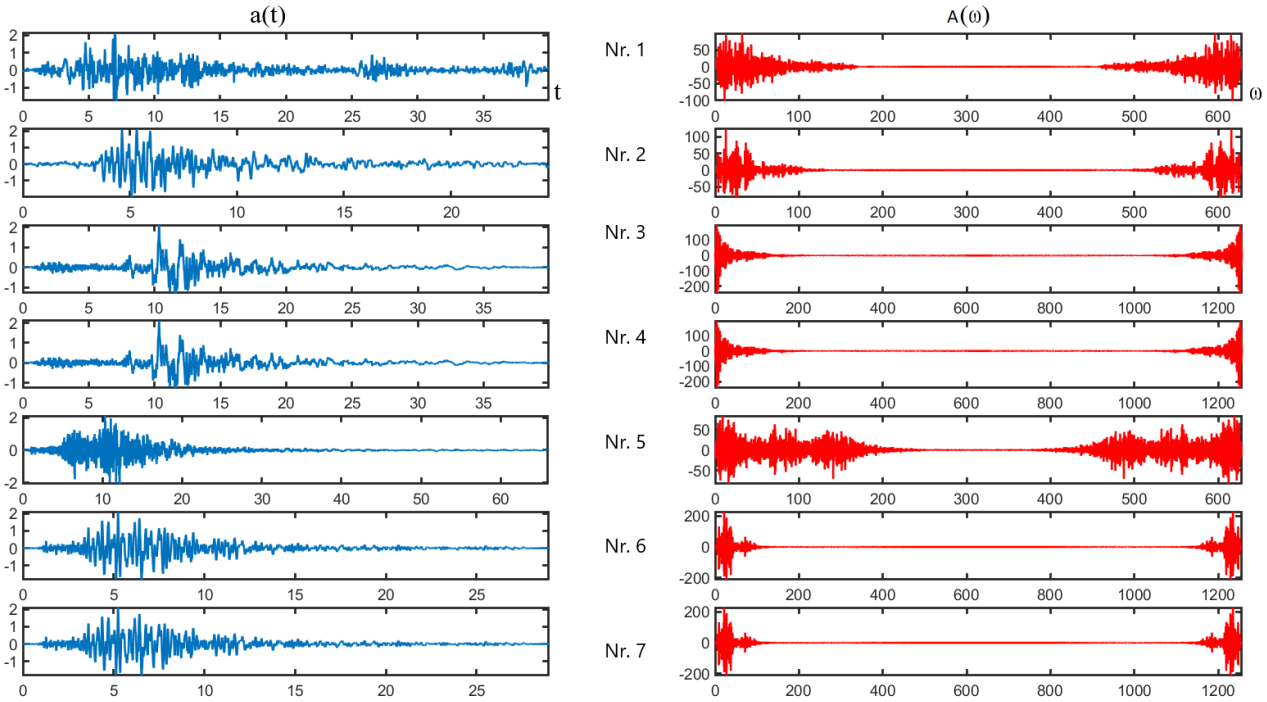

Figure 5. Real recorded spectra-compatible accelerograms. Group of 7 accelerograms is a valid input for dynamic analyses and evaluation of response spectra. Accelerograms are illustrated in time domain (x-axis in time[s]) and in frequency domain (x-axis in pulsation [rad/s]).

3.2 Case studies

Geotechnical quantities and model's parameters for soil are collected in Table 3. A local seismic response analysis has been performed and below the results are indicated as Case 0. This points out a resonance frequency at 10.18 rad/s. This value is the design parameter for the CF in metamaterial to use on the top of this type of soil. Indeed, seismic effects, without metamaterial, would be amplified dangerously at the resonance frequency of the soil, while a properly designed metamaterial, allows an attenuation of the seismic waves propagation due to the presence of the band-gap. The objective is to design internal local resonator to have a metamaterial with the bandgap including the most dangerous resonance frequency. As show equation (1.14), set design frequency, quantities k_i and m_i became design parameters.

$$\omega_r = \omega_i = \sqrt{\frac{k_i}{m_i}} \rightarrow k_i, m_i \qquad (1.14)$$

Starting from geometrical dimensions and mechanical characteristics of the experimental prototype (Casablanca et al., 2018), different case studies have been set by using as internal resonance frequency ω_r =10.18 rad/s. Numerical analyses of soil integrated with CF have been

performed to achieve solutions in time domain, frequency domain and response spectra. These calculations have been then compared with the results of Case 0.

Parameters for different case studies are indicated in Table 4.

3.3 Solution in time domain

The total horizontal acceleration at the top (the highest layer that model surface of the composite foundation) is represented for Case 1 in Figure 6. The solution shows reduction of most peaks of acceleration between Case 0 and Case 1. For the other case studies, the same result is noted.

3.4 Solution in frequency domain

In frequency domain, the transfer function is typically studied, calculated as ratio between the maximum acceleration at the layer of interest and the seismic input. Considering a decomposition of seismic forcing, the transfer function at the surface of the composite foundation (as can be seen from the ordering of the variables shown in and) is given by:

$$A(\omega_k) = \frac{\max(\ddot{u}_2(\omega_k))}{\max(a_g(\omega_k))}$$

Transfer function allows estimating attenuation capacity of devices used as a filter of some seismic frequencies.

The number of layers of the CF is another design parameter. Figures 7 and 8 illustrate the results for Case 1 (that are qualitatively equal to case 3) and Case 4 (that is qualitatively equal to case 2), obtained by varying the number of layers of CF. For the Case 1, reduction is non-monotonic as compared to Case 4. Indeed, Case 1 provides a little wider band-gap but the reduction of the first peak decreases with increasing of the number of layers while a reduction of the second peak is irregular. Another important aspect is the shift of the maximum amplification to lower frequencies. In reverse, Case 4 provides a considerable reduction of the first peak, there is no dangerous shift of the amplification to the left hand side of the axis of the frequencies, and the response to varying configuration is more regular. This reveals positive implications in the design process because of the setting of the parameters is easier and the attenuation effect is guaranteed even for various configurations.

Table 3. Parameters of study soil. Specific weight(γ), damping factor(D), total height(H) , shear wave velocity at surface(V_0) , heterogeneity coefficient and number of layers for one-dimensional discretization of volume of study soil.

γ (kN/mc)	D (%)	H (m)	N_{lay}	α	V_0 (m/s)
18	1	30	100	0.1	180

Table 4. Set of parameters for case studies used in numerical investigations. More cases have been chosen to evidence variability of dynamic response to varying geometry and mechanical parameters of device.

	m^e (kg)	m^i (kg)	k^e (N/m)	k^i (N/m)	N_{SM}
Case 1	317	245	$25.49 \cdot 10^3$	$155 \cdot 10^3$	4
Case 2	317	122.5	$12.74 \cdot 10^3$	$155 \cdot 10^7$	4
Case 3	634	490	$50.98 \cdot 10^3$	$310 \cdot 10^3$	4
Case 4	634	245	$25.49 \cdot 10^3$	$310 \cdot 10^7$	4

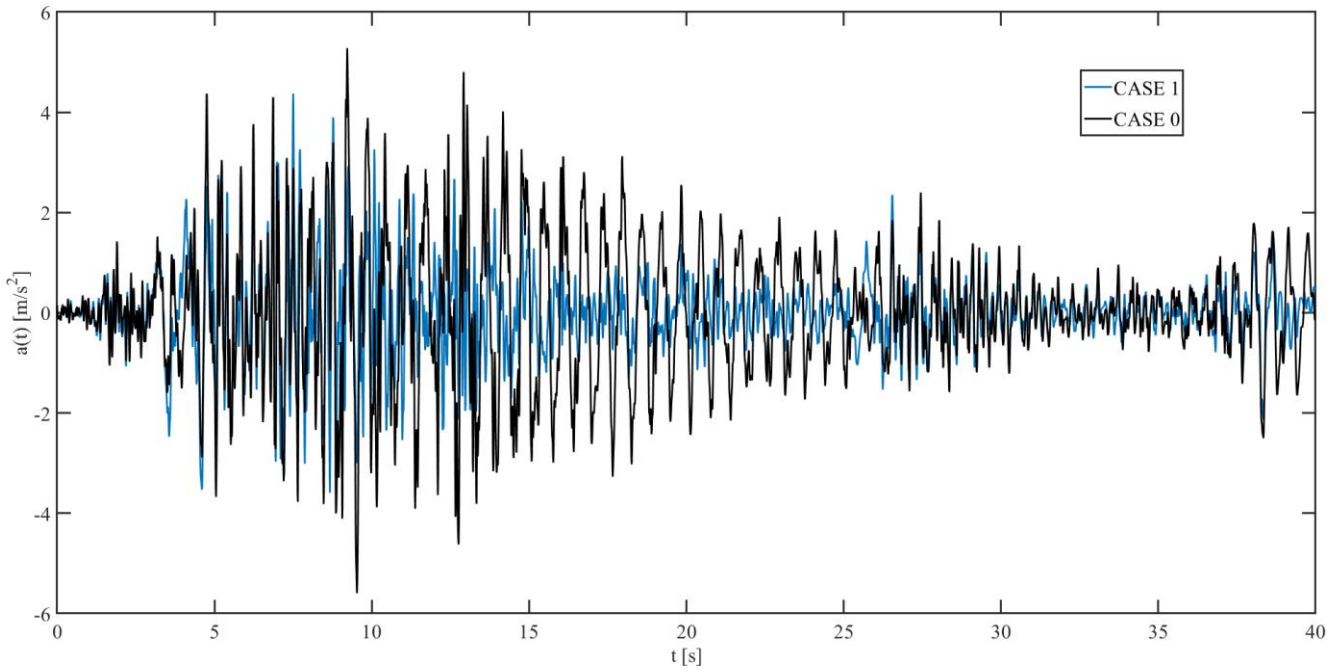

Figure 6. Horizontal acceleration at the top. In Case 1 the attenuation effect due to presence of the composite foundation is visible from the felling of most peaks.

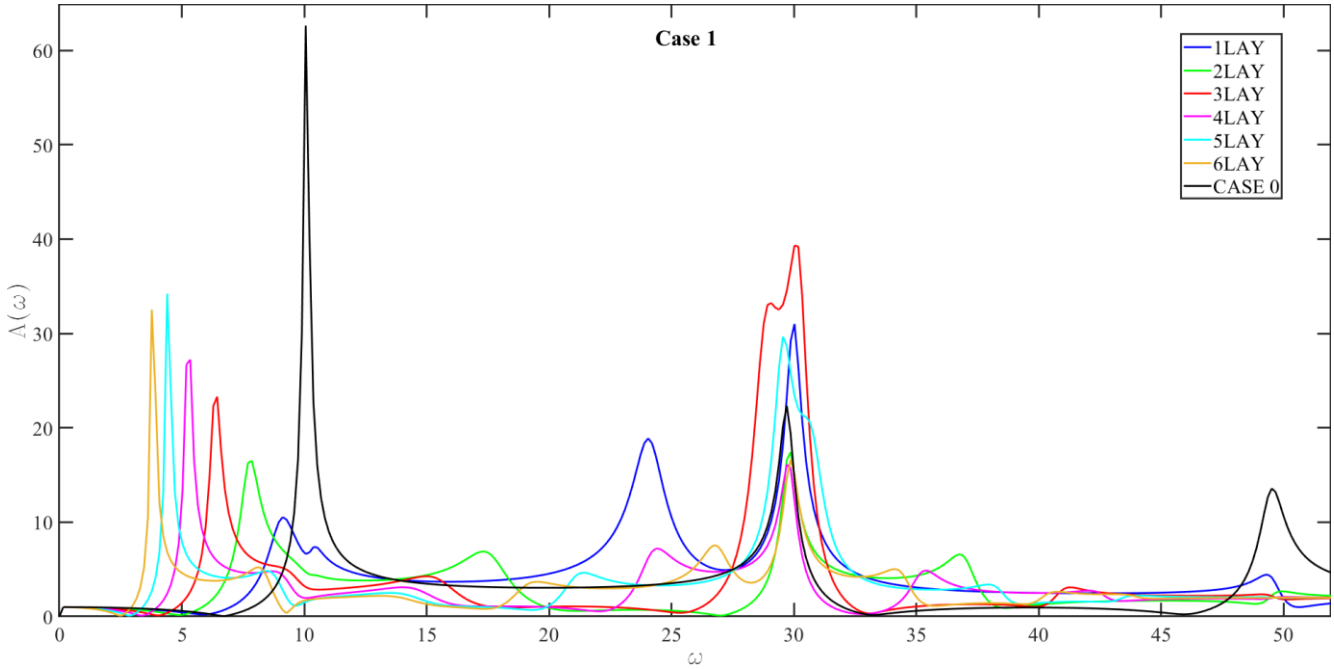

Figure 7. Transfer function for Case 1 by varying the number of layer of metamaterial, overlapped with Case 0.

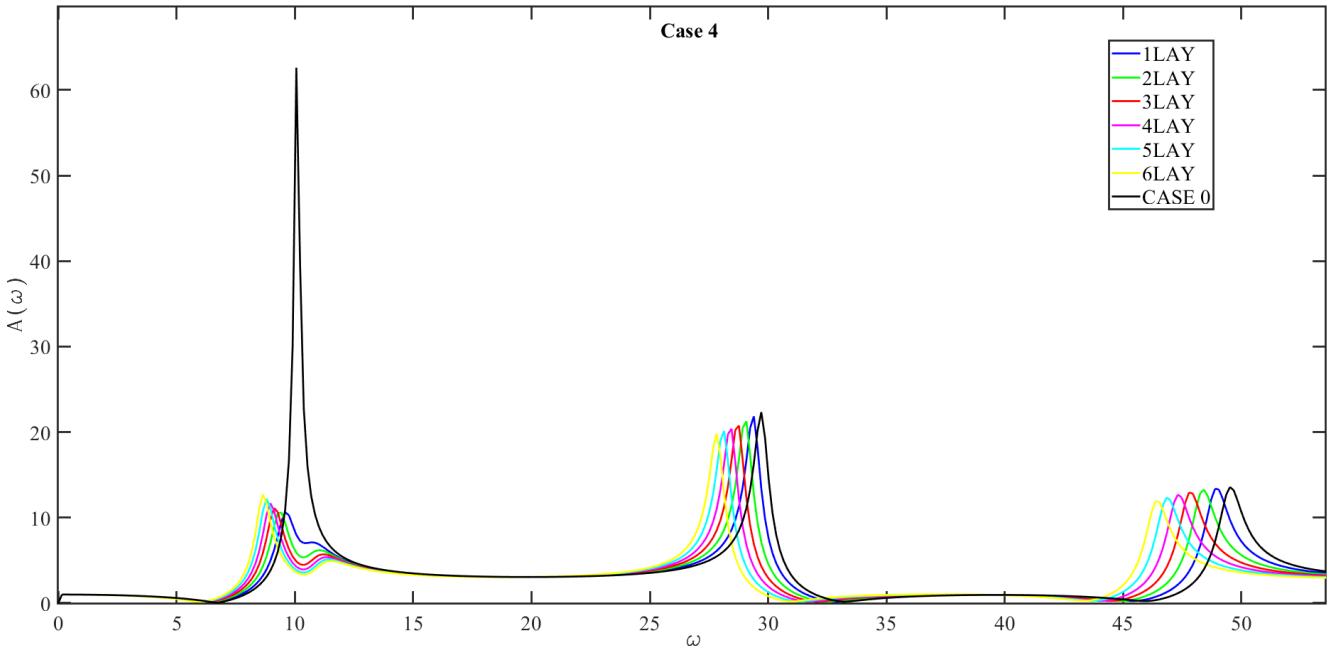

Figure 8. The transfer function for Case 4 by varying the number of layer of metamaterial, overlapped with Case 0.

3.5 Acceleration response spectra

The acceleration response spectra are the most used in the field of civil engineering design because spectral acceleration allows to directly evaluate the inertial force due to the design earthquake. Spectral acceleration, expressed in unit of *g* (gravity acceleration), means the maximum acceleration of one-dimensional harmonic oscillator with conventional damping equal to 5% (called in the following simple oscillator). Linear dynamic analysis has been performed by varying natural period of vibration of simple oscillator and collecting the maximum acceleration for each accelerogram of the set. In the end, an acceleration response spectrum is evaluated as an envelope of the results. Figure 9 illustrates envelope response spectra obtained for each case study by using the group of accelerograms representative of the design earthquake. Similarly to what has been observed in frequency domain, Both Cases 2 and 4 guarantee greater safety in the attenuation effect because reduction of the spectra is considerable starting from 0.1 s, although the maximum spectral acceleration is not reduced.

In Table 5, the parameters to compute the attenuation of response acceleration spectra are summarized: the maximum spectral acceleration (Sa,max) and the relative reduction percentage (SR,max); the spectral acceleration at high period (horizontal line) (Sa,h) and its reduction percentage (SR,h); the amplification ($A_{\omega r}$) at design resonance frequency and its reduction percentage (AR).

Table 5. Results summary. Comparison of acceleration response spectra and transfer function for each study cases. Comparisons are expressed in percentage also.

	Sa,max (g)	SR,max (%)	Sa,h (g)	SR,h (%)	$A_{\omega r}$	AR (%)
Case 0	1.82		1.28		62.62	
Case 1	1.52	16.52	1.16	9.74	27.23	56.52
Case 2	1.80	1.13	1.21	5.81	21.28	66.01
Case 3	1.54	15.26	1.14	10.98	32.02	48.87
Case 4	1.80	1.13	1.09	14.99	20.40	67.42

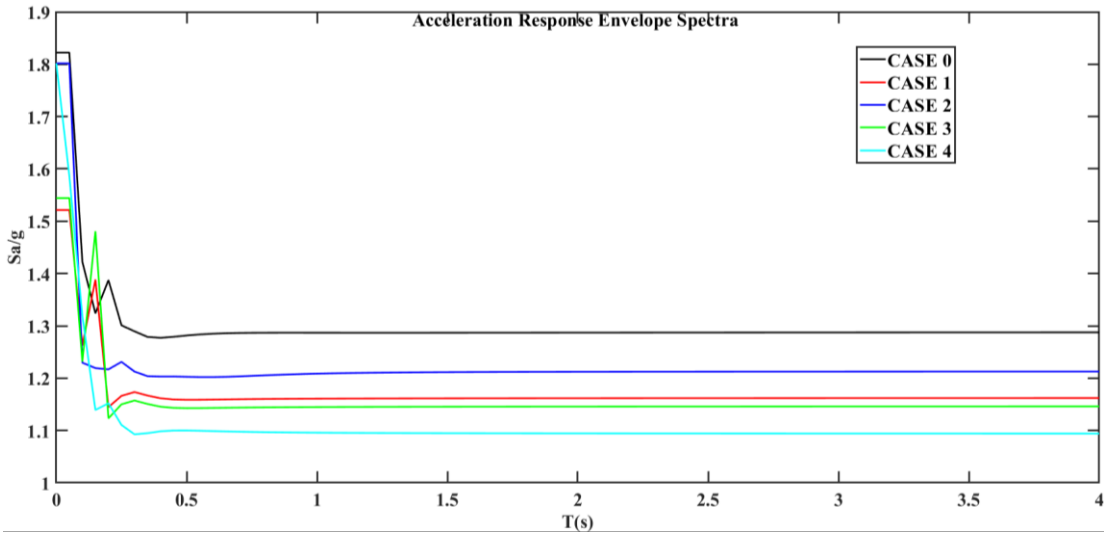

Figure 9. Acceleration response envelope spectra for each case studies in comparison with Case 0.

4 CONCLUSIONS

A simplified one-dimensional mechanical model is applied to integrate CF in the soil modeling with lumped parameters. A dynamic solution is studied in time and frequency domain and the main results are illustrated to estimate the attenuation capacity of the CF. Geometric parameters of CF are chanced to investigate the different behavior of the system and some particularities are evidenced.

The main concept is that the CF can be designed to act as a filter for the most dangerous frequencies for the building. Design parameters are the geometries of the concrete plates and steel internal cylinders. This technology shows a promising strategy for modern seismic protection of the buildings.

5 REFERENCES

Anil K. Chopra. (2013). *Dynamics of Structures.Theory and Applications to Earthquake Engineering.* Pearson.

Casablanca, O., Ventura, G., Garescì, F., Azzerboni, B., Chiaia, B., Chiappini, M., & Finocchio, G. (2018). Seismic isolation of buildings using composite foundations based on metamaterials. *Journal of Applied Physics*,**123**,174903

Chatzi, E. N., Dertimanis, V. K., Antoniadis, I. A., & Wagner, P. R. (2016). On the feasibility of structural metamaterials for seismic-induced vibration mitigation. *International Journal of Earthquake and Impact Engineering*, Vol. **1** Nos.1/2.

Corigliano, M., Lai, C. G., Rota, M., & Strobbia, C. L. (2012). ASCONA: Automated selection of compatible natural accelerograms. *Earthquake Spectra*, Vol. **28**, pp. 965–987.

Finocchio, G., Casablanca, O., Ricciardi, G., Alibrandi, U., Garescì, F., Chiappini, M., & Azzerboni, B. (2014). Seismic metamaterials based on isochronous mechanical oscillators. *Applied Physics Letters*,**104**,191903.

Giuseppe Lanzo, F. S. (1999). *Risposta sismica locale.Teoria ed esperienze.*Hervelius.

Huang, H. H., & Sun, C. T. (2009). Wave attenuation mechanism in an acoustic metamaterial with negative effective mass density. *New Journal of Physics*, ***11***,*013003*.

Huang, H. H., Sun, C. T., & Huang, G. L. (2009). On the negative effective mass density in acoustic metamaterials. *International Journal of Engineering Science*, ***47***,610–617.

Kramer, Steven L. (1996). *Geothecnical Earthquake Engineering.*Pearson.

Lanzo, G., Pagliaroli, A., & D'Elia, B. (2003). Numerical study on the frequency-dependent viscous damping in dynamic response analyses of ground. *Advances in Earthquake Engineering*, ***13***, 315–324.

Lo Presti, D. C., Lai, C. G., & Puci, I. (2006). ONDA: Computer Code for Nonlinear Seismic Response Analyses of Soil Deposits. *Journal of Geotechnical and Geoenvironmental Engineering*, ***132***(2), 223–236.

Robert A. Witte. (1993). *Spectrum&Network Measurements.* Hewlett Packard Company.

Tan, K. T., Huang, H. H., & Sun, C. T. (2012). Optimizing the band gap of effective mass negativity in acoustic metamaterials. *Applied Physics Letters*, ***101***,241901.

Zhou, Y., Wei, P., & Tang, Q. (2016). Continuum model of a one-dimensional lattice of metamaterials. *Acta Mechanica*, ***227***(8), 2361–2376.